Chinese Chemical Letters 34 (2023) 107663

Contents lists available at ScienceDirect

Chinese Chemical Letters

journal homepage: www.elsevier.com/locate/cclet

Linker optimization of HEPT derivatives as potent non-nucleoside HIV-1 reverse transcriptase inhibitors: From S=O to CHOR

Qingqing Hao[a], Xu Ling[a], Christophe Pannecouque[d], Erik De Clercq[d], Fener Chen[a,b,c,*]

[a] Sichuan Research Center for Drug Precision Industrial Technology, West China School of Pharmacy, Sichuan University, Chengdu 610041, China
[b] Department of Chemistry, Engineering Center of Catalysis and Synthesis for Chiral Molecules, Fudan University, Shanghai 200433, China
[c] Shanghai Engineering Center of Industrial Asymmetric Catalysis for Chiral Drugs, Shanghai 200433, China
[d] Rega Institute for Medical Research, KU Leuven, Herestraat 49, Leuven B-3000, Belgium

ARTICLE INFO

Article history:
Received 25 May 2022
Revised 30 June 2022
Accepted 5 July 2022
Available online 8 July 2022

Keywords:
HIV
NNRTIs
HEPTs
RT
Optimization

ABSTRACT

A novel series of CHOR-HEPT non-nucleoside HIV-1 reverse transcriptase inhibitors were developed by means of structure-based design strategy based on compound **6** reported previously by our group. Most of these compounds showed moderate to good activity toward wild-type HIV-1 strain with EC_{50} values in the range of 0.18–51.88 μmol/L and SI values in the range of 4–907. The compound **14aj** with a CHOH linker and compound **13i** with a CHOTMS linker in this series exhibited improved anti-HIV-1 activity (EC_{50} = 0.18 μmol/L, and 0.20 μmol/L) with higher selectivity (SI = 907, and 665) as comparison with the lead compound **6** (EC_{50} = 0.59 μmol/L, SI = 9). These two compounds **14aj** and **13i** were more sensitive than **6** toward clinically relevant mutant L100I, K103N and E138K viruses, which were further evaluated for their activity against wild-type reverse transcriptase and displayed a good correlation with the cell-based activity. Preliminary molecular modeling investigations provided insight for further structural optimization of HEPT.

Acquired immune deficiency syndrome (AIDS) was identified in 1981 [1]. It is characterized by human immunodeficiency virus (HIV) infection leading to $CD4^+$ T cell depletion and resulting in severe immunosuppression and increased incidence of opportunistic infections [2]. Globally, 1.1–2.1 million people were newly infected with HIV and about 480,000 to 1.0 million patients died of AIDS-related illnesses in 2020 based on data from the Joint United Nations Program on HIV/AIDS (UNAIDS) report [3]. HIV-1 is a retrovirus that utilizes the reverse transcriptase (RT) enzyme to convert the viral single-stranded RNA into double-stranded DNA. RT-targeted drugs can be divided into nucleoside (acid) RT inhibitors (NRTIs) and non-nucleoside RT inhibitors (NNRTIs). As an integral part of standard therapy in highly active antiretroviral therapy (HAART) regimens, NNRTIs are highly sought after due to their high antiviral potency, relatively low toxicity, and favorable pharmacokinetic properties. To date, eight NNRTIs have been approved for the treatment of HIV in the clinic, including Nevirapine (NVP), Delavirdine (DLV), Efavirenz (EFV), Etravirine (ETR), Rilpivirine (RPV), Elsulfavirine (ELV), Doravirine (DOR) and Ainuovirine (ANV) [4,5]. However, the rapid emergence of drug resistance and severe side effects of long-term administration has motivated medicinal chemists to develop a variety of potent NNRTIs with superior drug resistance and improved drug-like properties [6,7].

The 1-[(2-hydroxyethoxy)methyl]-6-(phenylthio)thymine (HEPT, Fig. 1), reported by Miyasaka and colleagues in 1989 as a kind of NNRTIs, showed moderate antiviral activity (EC_{50} = 7 μmol/L) and weak selectivity index (SI = 106) [8]. Over the past three decades, considerable efforts have been made in the structural optimization of HEPT, leading to the identification of MKC442, a Phase III clinical drug candidate, which was unfortunately terminated due to its undesirable metabolic properties [9]. Our research group focuses on the discovery of anti-HIV drugs and has performed many kinds of structural modifications on the unique structure of HEPT. Several naphthyl-containing HEPT analogs, such as compounds **3–5**, were found to show potent inhibitory activity against WT HIV-1 (Fig. 1), but their activity toward clinically relevant mutants has not been determined [10–14]. Recently, we have developed a series of novel sulfinyl-containing HEPT analogs through a structure-based drug design strategy. The representative compound **6** in this series showed improved inhibitory activity (EC_{50} = 0.59 μmol/L) but with an extremely poor selectivity index (SI = 9), compared to HEPT [15]. In addition, it was still inactive toward clinically relevant mu-

* Corresponding author at: Department of Chemistry, Engineering Center of Catalysis and Synthesis for Chiral Molecules, Fudan University, Shanghai 200433, China.
E-mail address: rfchen@fudan.edu.cn (F. Chen).

https://doi.org/10.1016/j.cclet.2022.07.006
1001-8417/

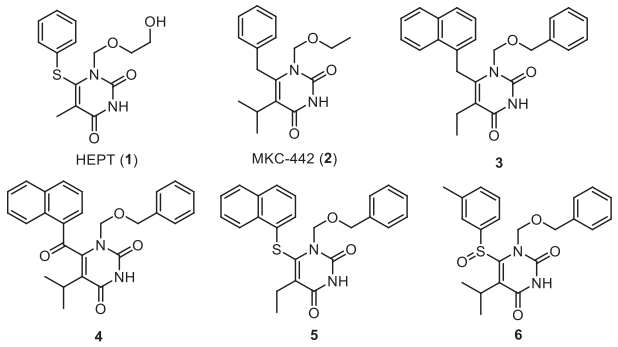

Fig. 1. The structures of HEPT and its analogs.

tants. Therefore, further structural optimization is still needed to find more safe and effective drug candidates.

In the present study, we endeavored to optimize compound **6** by introducing CH-OH and CH-OTMS groups into the linker, respectively, aiming to further extend the SAR of HEPTs. The predicted docking studies of **6** with RT indicated that the central thymine skeleton of **6** was oriented by two hydrogen bonds between CONH moiety and the protein (Fig. 2B): (i) a hydrogen bond between the NH of thymine and the carbonyl oxygen of K101; (ii) a water-mediated hydrogen bond between the NH of thymine and K101. The C6-phenyl ring of **6** was directed toward the hydrophobic aromatic pocket and formed π-π and hydrophobic interactions with W229, Y188 and Y181 residues, respectively. However, when the S=O linker of **6** was replaced with a CH-OH linker (**14i**), the orientation of the oxygen changed compared to **6** (Fig. 2C). The CH-OH linker would allow the molecule to retain good molecular flexibility and adopt multiple conformations within the NNIBP, which may be beneficial for being sensitive to mutant variations [13,16,17]. In addition, our previous work revealed that the CH-OH linker region was a typical metabolic site in DAPYs, which was responsible for

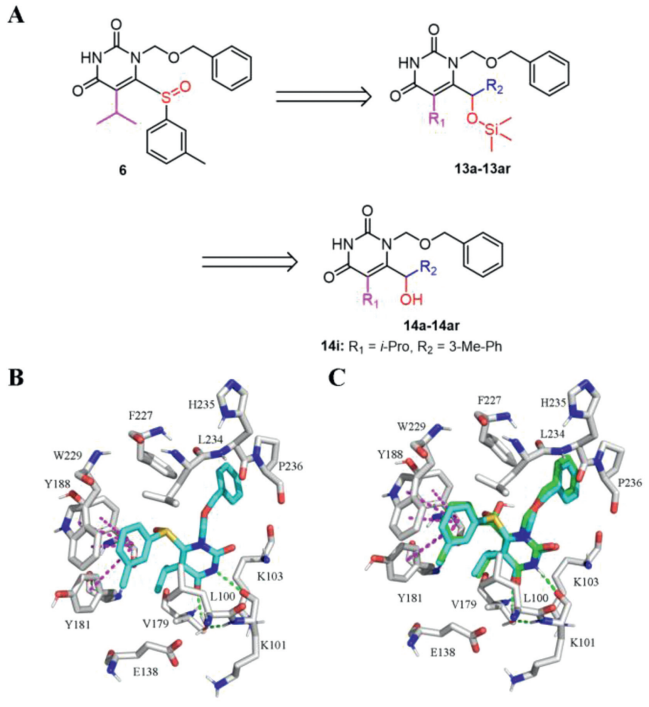

Fig. 2. (A) Design of target compounds based on the lead compound **6**; (B) Predicted binding model of **6** (blue) with RT (PDB: 1RT2); (C) Overlay of **14i** (green) and **6** (blue) within the binding pocket of RT.

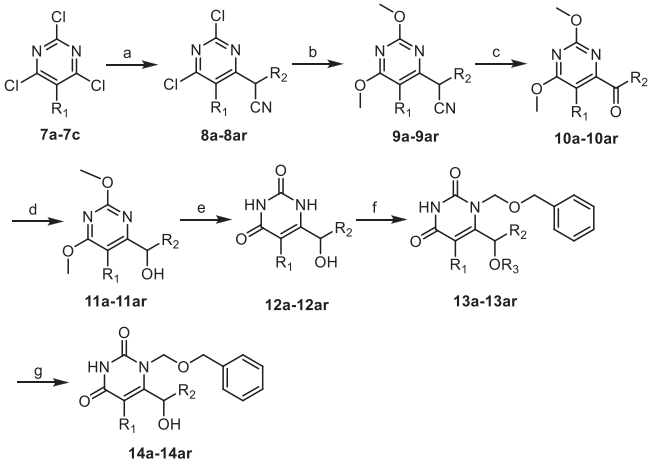

Scheme 1. Reagents and conditions: (a) NaH, substituted cyanides, DMF, −10 °C - r.t., overnight; (b) NaOMe, MeOH, reflux, 12 h; (c) NaH, O_2, THF, −10 °C - r.t., overnight; (d) $NaBH_4$, MeOH, r.t., 2–4 h; (e) conc. HCl, MeOH, reflux, overnight; (f) BSA, TBAI, benzyl chloromethyl ether, DCM, r.t., 4 h; (g) TBAF, THF, r.t., 0.5 h.

their poor metabolic stability [18]. The introduction of a silicon atom to a known drug molecule can lead to significant changes in drug biological activity and metabolism [19]. For example, the introduction of a (trimethylsilyl)ethyl group into camptothecin significantly improved its broad-spectrum anticancer activity, and enhanced tissue penetration as well as bioavailability [20]. In addition, cytarabine was an anti-metabolite that is converted into a prodrug through one or more silicon-based protecting groups with improved lipophilicity [21]. Therefore, CH-OTMS-containing HEPT analogs as intermediates of CH-OH compounds were also investigated.

The synthetic route to targeted molecules **14a-14ar** was depicted in Scheme 1. The nucleophilic substitution of trichloropyrimidines **7a-7c**, prepared according to our previously reported protocol [15], with appropriate cyanides was conducted using sodium hydride as base in dry DMF, producing corresponding dichloropyrimidines **8a-8ar**, as previously described by Loksha and coworkers [22]. Treating **8a-8ar** with NaOMe in MeOH at 65 °C for 12 h afforded dimethoxypyrimidines **9a-9ar**, which were then subjected to oxidation reaction by oxygen atmosphere in the presence of NaH in anhydrous THF to provide carbonyl pyrimidines **10a-10ar**. **10a-10ar** were reduced by $NaBH_4$ in MeOH at room temperature for 2–4 h to furnish alcohols **11a-11ar** [23]. Demethylation of **11a-11ar** with conc. HCl in MeOH at 65 °C overnight delivered thymine analogs **12a-12ar**, which were next treated with benzyl chloromethyl ether in the presence of *N*,*O*-bis(trimethylsilyl)acetamide (BSA) and tetrabutylammonium iodide (TBAI) in DCM at room temperature for 4 h to afford **13a-13ar**. Deprotection of **13a-13ar** with TBAF in THF at room temperature for 0.5 h finally yielded desired products **14a-14ar** in 68%–93% yields.

All the target compounds were evaluated for their *in vitro* anti-HIV activity and cytotoxicity in MT-4 cells infected with the WT HIV-1 (III_B). The preliminary biological results were summarized in Table 1, taking compound **6**, HEPT, NVP, and EFV as controls. Molecular docking was performed using Schrödinger Maestro 11.4 software to predict the binding modes of selected compounds to RT, the docking results of which were visualized and generated by PyMOL. When the linker was CH-OH, we explored the effect of the position and diversity of substituents on the R_2 phenyl ring on antiviral activity (**14a-14y**). The results in Table 1 indicated that most of these compounds showed moderate to good activity toward wild-type HIV-1 strain with EC_{50} values ranging from 0.22 μmol/L to 47.76 μmol/L and selectivity index (SI) in the range of 2–446.

Table 1
Activity and cytotoxicity of the target compounds against HIV-1 (III_B) in MT-4 cells.

Compd.	R_1	R_2	EC_{50} (μmol/L)[a]	CC_{50} (μmol/L)[b]	SI[c]	Compd.	R_1	R_2	EC_{50} (μmol/L)[a]	CC_{50} (μmol/L)[b]	SI[c]
6			0.59 ± 0.21	5.09 ± 0.96	9	**14t**	*i*-pro	3,5-diF-Ph	0.33 ± 0.09	28.27 ± 5.35	85
13d	*i*-pro	Ph	27.50 ± 21.42	>276.17	>10	**14u**	*i*-pro	3-F, 5-OMe-Ph	0.86 ± 0.13	35.73 ± 3.51	42
13i	*i*-pro	3-Me-Ph	0.20 ± 0.03	133.14 ± 18.74	665	**14v**	*i*-pro	3,5-diOMe -Ph	3.38 ± 0.31	147.87 ± 9.58	44
13j	*i*-pro	4-Me-Ph	>267.87	>267.87		**14w**	*i*-pro	4-BiPh	>25.70	25.70 ± 2.53	<1
13k	*i*-pro	2-F-Ph	1.39 ± 0.35	>265.61	>191	**14x**	*i*-pro	α-Naphthyl	1.15 ± 0.13	30.61 ± 1.46	27
13l	*i*-pro	3-F-Ph	>265.61	>265.61		**14y**	*i*-pro	β-Naphthyl	>32.95	32.95	<1
13q	*i*-pro	3-Br-Ph	>235.17	>235.17		**14z**	Me	2-Me-Ph	48.76 ± 6.01	181.79 ± 11.86	4
13s	*i*-pro	3-CF_3-Ph	>240.10	>240.10		14aa	Me	3-Me-Ph	5.50 ± 1.19	179.09 ± 5.98	33
13w	*i*-pro	3,5-diF-Ph	33.64 ± 9.96	>255.17	>8	**14ab**	Me	4-Me-Ph	>168.58	168.58	<1
13ah	Me	Ph	>32.51	32.51	<1	**14ac**	Me	3-F-Ph	19.94 ± 2.44	185.16 ± 5.81	9
14a	*i*-pro	Ph	1.12 ± 0.25	105.09 ± 28.77	94	**14ad**	Me	4-F-Ph	>114.95	114.95	<1
14b	*i*-pro	2-OMe-Ph	0.96 ± 0.23	139.53 ± 24.48	146	**14ae**	Me	2-OMe-Ph	51.88 ± 8.23	221.22 ± 14.83	4
14c	*i*-pro	3-OMe-Ph	2.36 ± 0.62	304.53	>129	**14af**	Me	3-OMe-Ph	38.40 ± 9.01	178.41 ± 9.49	5
14d	*i*-pro	4-OMe-Ph	47.76 ± 2.10	71.92 ± 6.70	2	**14ag**	Me	4-OMe-Ph	>165.95	165.95	<1
14e	*i*-pro	2-OCF_3-Ph	4.28 ± 0.92	>269.14	>63	**14ah**	Me	Ph	47.25 ± 9.30	180.53 ± 13.70	4
14f	*i*-pro	3-OCF_3-Ph	16.13 ± 7.44	>269.14	>17	**14ai**	Et	2-Me-Ph	3.52 ± 1.38	178.77 ± 3.44	51
14g	*i*-pro	4-OCF_3-Ph	>28.09	28.09	<1	**14aj**	Et	3-Me-Ph	0.18 ± 0.04	166.64 ± 24.86	907
14h	*i*-pro	2-Me-Ph	1.19 ± 0.35	177.14 ± 88.89	149	**14ak**	Et	4-Me-Ph	32.58 ± 8.91	160.12 ± 178.45	5
14i	*i*-pro	3-Me-Ph	0.22 ± 0.02	96.04 ± 29.87	446	**14al**	Et	2-F-Ph	2.44 ± 0.78	160.38 ± 11.51	66
14j	*i*-pro	4-Me-Ph	>37.66	37.66 ± 4.46	<1	**14am**	Et	3-F-Ph	0.55 ± 0.10	176.82 ± 7.20	319
14k	*i*-pro	2-F-Ph	1.07 ± 0.24	113.40 ± 39.80	106	**14an**	Et	4-F-Ph	43.02 ± 8.73	165.74 ± 10.48	4
14l	*i*-pro	3-F-Ph	0.44 ± 0.09	61.03 ± 11.56	140	**14ao**	Et	2-OMe-Ph	1.03 ± 0.24	168.90 ± 7.77	163
14m	*i*-pro	4-F-Ph	>29.31	>29.31		**14ap**	Et	3-OMe-Ph	1.69 ± 0.35	171.88 ± 4.88	102
14n	*i*-pro	2-Cl-Ph	0.50 ± 0.08	61.31 ± 20.72	122	**14aq**	Et	4-OMe-Ph	>160.66	160.66	<1
14o	*i*-pro	3-Cl-Ph	0.48 ± 0.10	59.01 ± 3.45	124	**14ar**	Et	Ph	1.29 ± 0.23	182.69 ± 7.04	142
14p	*i*-pro	4-Cl-Ph	>29.77	>29.77		HEPT[d]			7.0	740	106
14q	*i*-pro	3-Br-Ph	0.68 ± 0.11	51.73 ± 5.86	76	NVP			0.17 ± 0.06	>15.02	>91
14r	*i*-pro	4-Br-Ph	>28.80	28.80 ± 0.67	<1	EFV			0.003±0.001	>6.336	>2143
14s	*i*-pro	3-CF_3-Ph	3.06 ± 0.44	92.58 ± 36.67	30						

[a] EC_{50}: The effective concentration of the test compound required to protect MT-4 cells against HIV-induced cytopathogenicity by 50%.
[b] CC_{50}: The cytotoxic concentration of the test compound that reduced the normal uninfected MT-4 cell viability by 50%.
[c] SI: Selectivity index, ratio CC_{50}/EC_{50} (WT).
[d] HEPT: The data were obtained from the same laboratory (Prof. Erik De Clercq, Rega Institute for Medical Research, KU Leuven, Belgium) with the same method [24].

Among them, the most active compound **14i** exhibited significantly enhanced efficacy toward wild-type HIV-1 ($EC_{50} = 0.22$ μmol/L), which was about 3-fold more potent than compound **6**. The cytotoxicity of **14i** was also improved with a much higher selectivity index (SI = 446) than **6** (SI = 9). Introduction of bulky substituents at the *meta*-position of the phenyl ring was detrimental to anti-HIV activity such as **14c**, **14f** and **14s**. Besides, the introduction of different functional groups to the *para*-position of the benzene ring resulted in decreased antiviral activity (**14d**, **14g**, **14j**, **14m**, **14p**, **14r**, **14w**). For the mono-halogen-substituted compounds, the position priority abided by the rules as follows: *meta-* > *ortho-* > *para-*, for example, **14l** > **14k** > **14m**, **14o** > **14n** > **14p**, **14q** > **14r**. For these compounds with electron-donating group, their inhibitory activity mostly abided by the rules as follows: *ortho-* > *meta-* > *para-* (**14b** > **14c** > **14d**, **14e** > **14f** > **14g**), whereas introducing a methyl group at *meta*-position on benzene ring (**14i**) led to the best anti-HIV-1 activity. Then, the di-substituted compounds were also investigated (**14t-14v**). The difluorinated compound **14t** exhibited more favorable anti-HIV-1 activity, compared to its monofluorinated analogs (**14k-14m**). However, enlarging the bulk of the substituent resulted in decreased anti-HIV-1 activity, such as **14t** > **14u** > **14v**. In addition, the substitution of the benzene ring with a naphthalene ring led to a 3-fold reduction in antiviral activity (**14x** *vs.* **14a**). Interestingly, the α-naphthyl substituent was more favorable for anti-HIV potency than β-naphthyl substituent (**14x** > **14y**).

Next, the effect of different sizes of R_1 substituent on the activity was also investigated. Comparing compounds **14a-14y** with **14z-14ah** in Table 1, substitution of the isopropyl group with a methyl group at C5 on the pyrimidine resulted in a significant reduction in antiviral activity. The isopropyl group was changed to ethyl group at C5 on pyrimidine (**14ai-14ar**), affording another potent compound **14aj**, which exhibited more potent antiviral activity ($EC_{50} = 0.18$ μmol/L) with higher SI value (SI = 907) than **14i**. In addition, some intermediates of **14a-14ar** were also evaluated for anti-HIV activity. The results illustrated in Table 1 showed that most of them exhibited decreased antiviral activity compared with their corresponding OH derivatives in **14a-14ar**, for instance, **14a** > **13a**, **14k** > **13k**, **14l** > **13l**, **14q** > **13q**, **14s** > **13s**, **14t** > **13t** and **14ah** > **13ah**. Exceptionally, **13i** exhibited comparable inhibitory activity ($EC_{50} = 0.20$ μmol/L) to **14i** ($EC_{50} = 0.22$ μmol/L, SI = 446), but the selectivity of **13i** was slightly improved (SI = 665).

Subsequently, **14i**, **14aa**, **14aj** and **13i** were selected to carry out molecular docking. As displayed in Fig. 3, **14i**, **14aj** and **14aa** fitted well into the binding pocket of NNIBP and formed crucial hydrogen bonding interactions and π-π interactions with surrounding residues. It was worth noting that **14aa** showed lower antiviral activity than **14i** and **14aj**, which may be due to the lack of π-π interaction with Y181. For **13i**, it showed different binding model compared with above three compounds. Not only did it form key hydrogen-bonding interactions and water-mediated hydrogen-bonding interactions with K101, but it also formed hydrogen-bonding interactions with K103 and π-π interactions with F227 and W229, resulting in enhanced activity.

Some representative compounds were selected to further evaluate their inhibitory activity toward a panel of clinically relevant drug-resistant HIV-1 mutant strains (L100I, K103N, and E138K) as described in Table 2. Pleasingly, **14i**, **14aj** and **13i** had superior activity to NVP toward K103N. **14i** and **13i** exhibited comparable potency to NVP toward E138K (EC_{50} < 1 μmol/L). The inhibitory activity of **14n** and **13k** against the L100I mutant was compara-

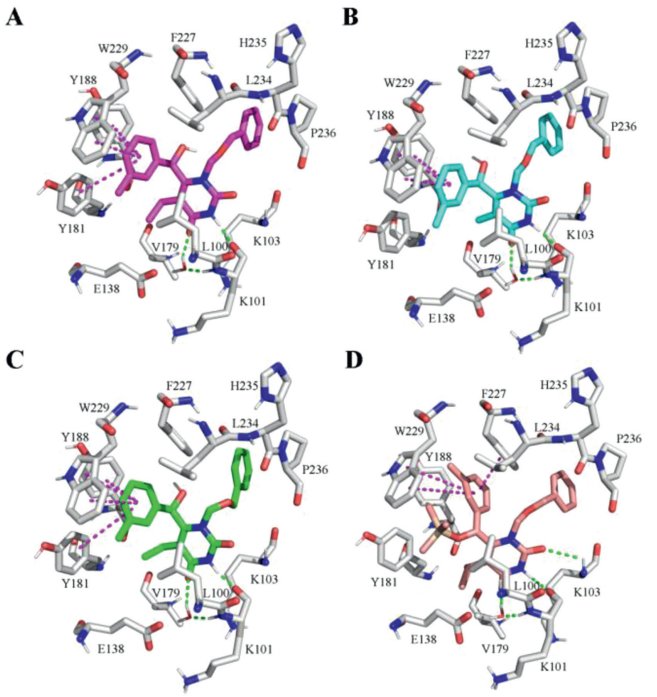

Fig. 3. Predicted binding models of the four selected compounds with wild-type HIV-1 RT (PDB: 1RT2) (A): **14i**, (B): **14aa**, (C): **14aj**, (D): **13i**.

ble to that of NVP. Thereafter, we performed site mutations at L100, K103, and E138 of WT HIV-1 RT by computational simulation. Five compounds (**14i**, **14k**, **14n**, **14aa** and **13i**) were selected to perform molecular docking with the mutant RT, respectively. The docking results illustrated in Fig. 4 revealed that the π-π stacking interaction with Y181 toward the L100I mutant strain was lost in **14aa**, interpreting the diminished activity of **14aa** (Figs. 4A and B). By comparing **14k** with **14aj**, we could hypothesize that **14aj** not only formed crucial hydrogen bonding interaction with K101 and water-mediated hydrogen bonding interaction with K101 but also formed hydrogen bonding interaction with N103, together resulting in higher K103N-associated mutant inhibitory than **14k**

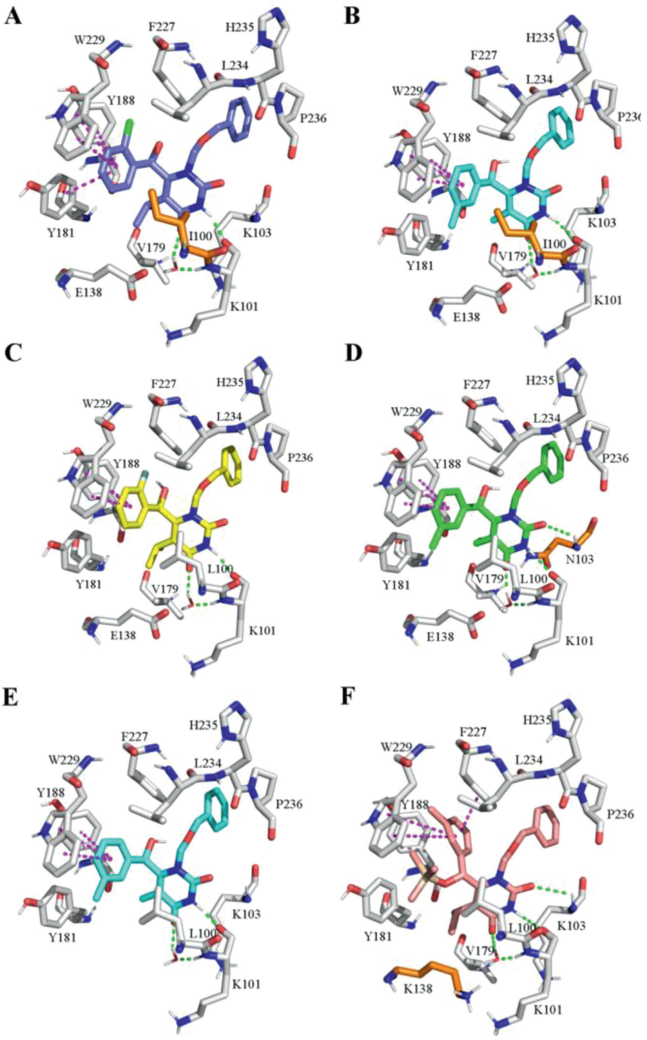

Fig. 4. Predicted binding models of the selected compounds with the mutant RT (PDB: 1RT2). (A) L100I with **14n**; (B) L100I with **14aa**; (C) K103N with **14k**; (D) K103N with **14aj**; (E) E138K with **14aa**; (F) E138K with **13i**. Mutated residues are depicted as orange sticks.

Table 2
Inhibitory activity of the selected compounds toward clinically relevant HIV-1 mutant strains.

Compd.	EC_{50} (μmol/L) [a]		
	L100I	K103N	E138K
13i	4.13 ± 1.48	5.19 ± 1.06	0.78 ± 0.13
13k	2.27 ± 0.78	>265.61	>237.41
14b	4.21 ± 0.30	>30.62	3.44 ± 0.46
14e	3.66 ± 1.66	30.54 ± 4.38	3.50 ± 0.82
14h	9.10 ± 0.46	63.03 ± 1.99	6.57 ± 2.55
14i	6.68 ± 5.12	6.67 ± 0.86	0.76 ± 0.17
14k	9.01 ± 7.80	39.06 ± 10.16	3.51 ± 0.64
14l	5.38 ± 2.21	>61.03	2.70 ± 0.79
14n	2.22 ± 1.16	>61.31	1.24 ± 0.27
14o	4.94 ± 1.28	11.17 ± 1.06	2.91 ± 0.65
14w	3.96 ± 1.14	9.57 ± 1.50	1.87 ± 0.45
14x	4.64 ± 1.93	>35.73	2.07 ± 0.62
14aa	25.81 ± 2.19	37.40 ± 4.69	25.26 ± 2.18
14aj	2.93 ± 0.94	3.88 ± 0.58	1.08 ± 0.22
14am	12.45 ± 4.92	9.57 ± 5.22	2.74 ± 0.66
14ao	4.30 ± 1.90	26.51 ± 6.75	3.92 ± 0.71
NVP	2.04 ± 0.64	7.66 ± 1.55	0.24 ± 0.14
EFV	0.018 ± 0.006	0.064 ± 0.031	0.003 ± 0.001

[a] EC_{50}: The effective concentration of the test compound required to protect MT-4 cells against HIV-induced cytopathogenicity by 50%.

(Figs. 4C and D). For the compound **14aa**, its efficiency was lower than **13i** and NVP, due to the deficiency of interaction with K103 toward the E138K mutant strain (Figs. 4E and F).

Furthermore, the representative compounds with good anti-HIV-1 activity were selected to evaluate their inhibitory activity toward WT HIV-1 RT to validate the binding target of these newly synthesized HEPTs (Table 3). All these tested compounds

Table 3
Inhibitory activity of the selected compounds against WT HIV-1 RT.

Compd.	IC_{50} (μmol/L)[a]	Compd.	IC_{50} (μmol/L)
13i	0.65 ± 0.02	**14o**	1.56 ± 0.33
14b	5.99 ± 1.19	**14q**	1.41 ± 0.21
14d	3.43 ± 0.66	**14s**	5.41 ± 1.07
14e	3.33 ± 1.40	**14u**	7.41 ± 0.70
14f	8.40 ± 2.41	**14w**	0.99 ± 0.02
14h	3.39 ± 1.09	**14x**	2.17 ± 0.11
14i	0.57 ± 0.12	**14aj**	1.23 ± 0.21
14k	5.16 ± 1.78	**14am**	3.62 ± 0.93
14l	1.69 ± 0.08	NVP	0.80 ± 0.16
14n	1.01 ± 0.15	EFV	0.011 ± 0.003

[a] IC_{50}: inhibitory concentration of the test compound required to inhibit WT HIV-1 RT polymerase activity by 50%.

displayed moderate inhibitory activity toward WT HIV-1 RT with IC_{50} values ranging from 0.57 μmol/L to 8.40 μmol/L. Among them, **14i** ($IC_{50} = 0.57$ μmol/L) and **13i** ($IC_{50} = 0.65$ μmol/L) showed the most potent activity against WT RT, being superior to NVP ($IC_{50} = 0.80$ μmol/L) but inferior EFV ($IC_{50} = 0.011$ μmol/L), which was consistent with their antiviral activity in MT-4 cells. The regression analysis of pEC_{50} and pIC_{50} displayed a good correlation ($R^2 = 0.8505$, Fig. S1 in Supporting information), indicating that these newly designed compounds could specifically bind to HIV-1 RT.

In conclusion, a novel series of structurally diverse CHOR-HEPT were synthesized and evaluated for their anti-HIV-1 activity. The majority of these compounds exhibited moderate to good activity against WT HIV-1 with EC_{50} values ranging from 0.18 μmol/L to 51.88 μmol/L and SI values ranging from 4 to 907. For OH-substituted compounds, the most active compound **14aj** with a CHOH linker displayed 3-fold increase in potency ($EC_{50} = 0.18$ μmol/L) toward WT HIV-1 and 100-fold improvement in selectivity (SI = 907), compared to the lead compound 6 ($EC_{50} = 0.59$ μmol/L, SI = 9). For CHOTMS-containing HEPT derivatives, compound **13i** with a CHOTMS linker exhibited comparable activity to **14aj** against WT HIV-1 ($EC_{50} = 0.20$ μmol/L) but with a slight decrease in selectivity (SI = 665). Pleasingly, both **13i** and **14aj** had moderate inhibitory activity toward clinically relevant mutant strains (L100I, K103N, and E138K). Besides, compound **13i** showed nanomolar inhibitory activity against WT RT ($IC_{50} = 0.65$ μmol/L) while **14aj** revealed low micromolar potency ($IC_{50} = 1.23$ μmol/L). The molecular docking studies were fully leveraged to explain the SARs. Our findings will lay the structural foundation for further structural optimization of HEPT. Continued efforts around the HEPT structural modifications are still on the way aiming to search for safer and more effective non-nucleoside HIV-1 reverse transcriptase inhibitors with good druggability.

Declaration of competing interest

The authors declare that they have no known competing financial interests or personal relationships that could have appeared to influence the work reported in this paper.

Acknowledgments

This work was financially supported by National Natural Science Foundation of China (No. 22077018) and National Key R&D Program of China (No. 2017YFA0506000). We thank Ningxia Medical University for providing the sources of molecular modeling.

Supplementary materials

Supplementary material associated with this article can be found, in the online version, at doi:10.1016/j.cclet.2022.07.006.

References

[1] R.C. Gallo, P.S. Sarin, E.P. Gelmann, et al., Science 220 (1983) 865–867.
[2] L.O. Kallings, J. Intern. Med. 263 (2008) 218–243.
[3] https://embargo.unaids.org/static/files/uploaded_files/UNAIDS_2021_FactSheet_en_em.pdf (accessed June 3, 2021).
[4] C.S. Adamson, E.O. Freed, Antivir. Res. 85 (2010) 119–141.
[5] R.D. Moore, R.E. Chaisson, AIDS 13 (1999) 1933–1942.
[6] R.K. Rawal, V. Murugesan, S.B. Katti, Curr. Med. Chem. 19 (2012) 5364–5380.
[7] Y. Mehellou, E.D. Clercq, J. Med. Chem. 53 (2010) 521–538.
[8] T. Miyasaka, H. Tanaka, M. Baba, et al., J. Med. Chem. 32 (1989) 2507–2509.
[9] N.R. El-Brollosy, P.T. Jørgensen, B. Dahan, et al., J. Med. Chem. 45 (2002) 5721–5726.
[10] G. Meng, F. Chen, E.D. Clercq, J. Balzarini, C. Pannecouque, Chem. Pharm. Bull. 51 (2003) 779–789.
[11] G. Sun, X. Chen, F. Chen, et al., Chem. Pharm. Bull. 53 (2005) 886–892.
[12] L. Ji, F. Chen, B. Xie, et al., Eur. J. Med. Chem. 42 (2007) 198–204.
[13] C. Zhuang, C. Pannecouque, E.D. Clercq, F. Chen, Acta Pharm. Sin. B 10 (2020) 961–978.
[14] P. Tang, H. Wang, W. Zhang, F. Chen, Green Synth. Catal. 1 (2020) 26–41.
[15] Q. Hao, S. Wang, W. Huang, et al., Bioorg. Chem. 126 (2022) 105880.
[16] K. Das, P.J. Lewi, S.H. Hughes, E. Arnold, Prog. Biophys. Mol. Biol. 88 (2005) 209–231.
[17] S. Gu, Q. He, S. Yang, et al., Bioorg. Med. Chem. 19 (2011) 5117–5124.
[18] X. Chen, L. Ding, Y. Tao, et al., Eur. J. Med. Chem. 202 (2020) 112549.
[19] J.S. Mills, G.A. Showell, Expert Opin. Investig. Drugs 13 (2004) 1149–1157.
[20] A.H.V. Hattum, H.M. Pinedo, H.M.M. Schlüper, et al., Int. J. Cancer 88 (2000) 260–266.
[21] W. Bains, J.G. Montana, WO Patent, WO2004050666 A1, 2004.
[22] Y.M. Loksha, E.B. Pedersen, R. Loddo, et al., J. Med. Chem. 57 (2014) 5169–5178.
[23] J. Zhu, M. Xin, C. Xu, et al., Acta Pharm. Sin. B 11 (2021) 3193–3205.
[24] H. Tanaka, H. Takashima, M. Ubasawa, et al., J. Med. Chem. 25 (1995) 2860–2865.